C.P. No. 1331

PROCUREMENT EXECUTIVE, MINISTRY OF DEFENCE

AERONAUTICAL RESEARCH COUNCIL

CURRENT PAPERS

Interference Problems on Wing-Fuselage Combinations Part 1; Lifting Unswept Wing attached to a Cylindrical Fuselage at Zero Incidence in Midwing Position

by

J. Weber

Aerodynamics Dept., R.A.E., Farnborough

LONDON: HER MAJESTY'S STATIONERY OFFICE

1975

PRICE £1-60 NET

UDC 533.695.12 : 533.693.2 : 533.696.3 : 533.6.011.32 :
533.6.048.3 : 533.6.041 : 518.1

CP No.1331*
July 1969

INTERFERENCE PROBLEMS ON WING-FUSELAGE COMBINATIONS PART I: LIFTING UNSWEPT WING ATTACHED TO A CYLINDRICAL FUSELAGE AT ZERO INCIDENCE IN MIDWING POSITION

by

J. Weber

SUMMARY

The incompressible flow field past a single straight vortex line which crosses a cylindrical circular fuselage at right angles has been studied. In particular the downwash induced in the plane through the vortex and the axis of the fuselage has been determined numerically.

The results are used to solve the design problem for an unswept wing of infinite aspect ratio for which the chordwise load distribution is given and the spanwise distribution in the presence of the fuselage is required to be constant. It is shown how the interference effect varies with the ratio R/c between the body radius and the wing chord, and with the spanwise distance from the junction.

A modification of existing methods (see e.g. Ref.3) for calculating the spanwise load distribution of wing-fuselage combinations is suggested to take account of the body interference with the chordwise load distribution.

---

* Replaces RAE Technical Report 69130 - ARC 31 532.

CONTENTS

1 INTRODUCTION

To study some of the interference effects between a fuselage and a lifting wing, we begin with a simple case in incompressible flow. We consider an infinite cylindrical fuselage of circular cross section with the axis parallel to the main stream. The isolated fuselage does thus not perturb the main stream. We consider an unswept lifting wing of constant chord and infinite span. The fuselage is attached to this wing in the midwing position.

The wing is supposed to have such a camber surface that it produces, with the fuselage present, a given chordwise load distribution which is constant along the span (i.e. chordwise and trailing vorticity occurs only far away from the fuselage and its effect is neglected near the fuselage).

The present investigation is to be of an accuracy similar to that of linear wing-theory, which means we may assume that the bound vortices lie in a plane, namely a plane through the axis of the fuselage. Each half of the wing is thus represented by a chordwise distribution of semi-infinite unswept vortex lines.

We are free to choose the way in which the vortices from one half of the wing are joined to the vortices from the other half. The vortices could, for example, run along the circumference of the fuselage. We take them such that we have infinite straight vortices in the gross wing plane.

To these vortices we must add singularity distributions either inside the fuselage or on its surface such that the total sum of the singularities produces zero normal velocity on the body surface, i.e. the fuselage remains to be a stream surface. We choose for the additional singularity distribution a source-sink distribution on the surface of the fuselage.

This source-sink distribution induces in the wing plane a normal velocity. The vortex distribution and its velocity field are the same as for the isolated wing, so that the total interference effect is given by the velocity field from the source-sink distribution.

We begin by considering a single vortex in the presence of the fuselage and determine the downwash field in the wing plane. From this we can then determine by a chordwise integration the downwash, i.e. the required camber, for a given chordwise load distribution. This means that in this paper we deal mainly with the design problem.

For the design problem, it seems sufficient to consider only a fuselage at zero incidence, since the design case is usually the cruise configuration, where the passenger cabin is at zero incidence. In this case, the effects of the nose and the rear of the fuselage on the flow over the wing can be approximated by those of the isolated fuselage.

The major aim of this paper is to elucidate certain interference effects. This is the reason for choosing a simple configuration, though the latter has no direct practical application.

The answers to the design problem can however be of some use when dealing with the problem to calculate the load distribution of a given wing in the presence of a fuselage. The framework used by Küchemann[1] to calculate the chord and spanwise load distribution for isolated wings can be extended to deal with wing-fuselage combinations.

Küchemann uses extensively the concept of a sectional life slope $a(y)$ which on a swept wing varies along the span. It seems justifiable to introduce for a straight wing attached to a fuselage a sectional lift slope which also varies along the span. This modification can easily be introduced into the method, developed by Multhopp[2] and extended in Ref.3, for calculating the spanwise load distribution on wing-fuselage combinations. Some results from the design problem can be used to determine the sectional lift slope $a(y)$ as function of the ratio of the body diameter and the wing chord.

2 SINGLE STRAIGHT VORTEX IN THE PRESENCE OF A CIRCULAR CYLINDRICAL FUSELAGE

2.1 Velocities induced by the vortex at the fuselage

Let x, y, z be a cartesian system of coordinates and x, r, ϑ a system of cylinder coordinates. We consider an infinite vortex through $x = 0, z = 0$ and parallel to the y-axis. The strength of the vortex is constant and equal to Γ. We consider further an infinitely long cylindrical fuselage of circular cross section $y^2 + z^2 = R^2 = 1$. The vortex crosses the fuselage thus at right angle.

The velocity field of the vortex has the components:

$$v_x = \frac{\Gamma}{2\pi} \frac{z}{x^2 + z^2}$$

$$v_y = 0$$

$$v_z = \frac{\Gamma}{2\pi} \frac{-x}{x^2 + z^2} \quad .$$

The vortex induces therefore at the surface of the fuselage a normal velocity component (positive outwards):

$$v_{n_1}(x,\vartheta) = v_y \cos\vartheta + v_z \sin\vartheta$$

$$= \frac{\Gamma}{2\pi} \frac{-x \sin\vartheta}{x^2 + \sin^2\vartheta} \quad . \tag{1}$$

The distribution of $-v_{n_1}(x,\vartheta)$ is illustrated in Fig.1.

2.2 Source distribution on the fuselage to make the fuselage a stream surface

This normal velocity can be cancelled by a source distribution of strength $q(x,\vartheta)$ on the surface of the fuselage.

A three-dimensional source Q at x', y', z' induces at x, y, z the velocity components

$$v_y = \frac{Q}{4\pi} \frac{y - y'}{\sqrt{(x - x')^2 + (y - y')^2 + (z - z')^2}^3}$$

$$v_z = \frac{Q}{4\pi} \frac{z - z'}{\sqrt{(x - x')^2 + (y - y')^2 + (z - z')^2}^3} \quad .$$

The source distribution $q(x,\vartheta)$ induces therefore at the cylinder the normal velocity

$$v_{n_2}(x,\vartheta) = \frac{q(x,\vartheta)}{2}$$

$$+ \int_{-\infty}^{\infty} \int_{0}^{2\pi} \frac{q(x',\vartheta')}{4\pi} \frac{[(\cos\vartheta - \cos\vartheta')\cos\vartheta + (\sin\vartheta - \sin\vartheta')\sin\vartheta]d\vartheta'dx'}{\sqrt{(x-x')^2 + (\cos\vartheta - \cos\vartheta')^2 + (\sin\vartheta - \sin\vartheta')^2}^3}$$

$$= \frac{q(x,\vartheta)}{2}$$

$$+ \int_{-\infty}^{\infty} \int_{0}^{2\pi} \frac{q(x',\vartheta')}{4\pi} \frac{[1 - \cos(\vartheta - \vartheta')]d\vartheta'dx'}{\sqrt{(x-x')^2 + 2[1 - \cos(\vartheta - \vartheta')]}^3} \quad . \tag{2}$$

To make the cylinder a stream surface we have to determine $q(x,\vartheta)$ such that

$$v_{n_2}(x,\vartheta) = - v_{n_1}(x,\vartheta) \quad . \tag{3}$$

Since

$$\int_{-\infty}^{\infty} \frac{[1 - \cos(\vartheta - \vartheta')]dx'}{\sqrt{(x - x')^2 + 2[1 - \cos(\vartheta - \vartheta')]}^3} = 1 \quad ,$$

we obtain from equations (1) to (3)

$$q(x,\vartheta) = \frac{\Gamma}{\pi} \frac{x \sin\vartheta}{x^2 + \sin^2\vartheta} - \int_0^{2\pi} \frac{q(x,\vartheta')}{2\pi} d\vartheta'$$

$$- \int_{-\infty}^{\infty} \int_0^{2\pi} \frac{[q(x',\vartheta') - q(x,\vartheta')][1 - \cos(\vartheta - \vartheta')]d\vartheta'dx'}{2\pi\sqrt{(x - x')^2 + 2[1 - \cos(\vartheta - \vartheta')]}^3} \quad .$$

The source distribution $q(x,\vartheta)$ has the same planes of symmetry or anti-symmetry as $v_{n_1}(x,\vartheta)$:

$$\begin{aligned} q(x,\vartheta) &= - q(-x,\vartheta) \\ &= - q(x,-\vartheta) \\ &= q(x, \pi - \vartheta) \quad . \end{aligned}$$

As a consequence

$$\int_0^{2\pi} q(x,\vartheta)d\vartheta = 0 \quad .$$

The source distribution has therefore to satisfy the equation:

$$q(x,\vartheta) = \frac{\Gamma}{\pi} \frac{x \sin\vartheta}{x^2 + \sin^2\vartheta}$$

$$- \int_{-\infty}^{\infty} \int_0^{2\pi} \frac{[q(x',\vartheta') - q(x,\vartheta')][1 - \cos(\vartheta - \vartheta')]d\vartheta'dx'}{2\pi\sqrt{(x - x')^2 + 2[1 - \cos(\vartheta - \vartheta')]}^3} \quad . \tag{4}$$

A numerical solution of this equation could be determined in a manner similar to the method developed by A.M.O. Smith and J.L. Hess (see, for example, Ref.4) for calculating the pressure distribution on a non-lifting wing-fuselage combination. This would however involve the solution of a large system of linear equations.

Our aim was to determine only an approximate solution but with somewhat less effort. Further we intended to deal with continuous functions for the source distribution, instead of using panels of constant source strength, since with the latter one obtains realistic results only for certain points on the panels. This is particularly important, since we wanted to perform the lengthy part of the calculation (i.e. the determination of the source distribution on the fuselage and the downwash which the latter induces in the wing plane) only once namely for a single vortex and then use the results with a series of chordwise vortex distributions $\gamma(x)$.

Equation (4) can also be solved by an iteration procedure, such that the nth approximation $q^{(n)}(x,\vartheta)$ is derived from the $(n-1)$th approximation by

$$q^{(n)}(x,\vartheta) = \frac{\Gamma}{\pi}\frac{x \sin\vartheta}{x^2 + \sin^2\vartheta} - \int_{-\infty}^{\infty}\int_{0}^{2\pi} \frac{\left[q^{(n-1)}(x',\vartheta') - q^{(n-1)}(x,\vartheta')\right]\left[1 - \cos(\vartheta - \vartheta')\right] d\vartheta' dx'}{2\pi\sqrt{(x - x')^2 + 2\left[1 - \cos(\vartheta - \vartheta')\right]^3}} .$$

We note first that the approximation

$$q^{(0)}(x,\vartheta) = \frac{\Gamma}{\pi}\frac{x \sin\vartheta}{x^2 + \sin^2\vartheta} \tag{5}$$

represents the approximation according to slender theory, for which we would solve at each station x the corresponding two-dimensional problem.

We have performed only the next step in the iteration procedure and calculated $q^{(1)}(x,\vartheta)$ from

$$q^{(1)}(x,\vartheta) = \frac{\Gamma}{\pi}\frac{x \sin\vartheta}{x^2 + \sin^2\vartheta} - \int_{-\infty}^{\infty}\int_{0}^{2\pi} \frac{\left[q^{(0)}(x',\vartheta') - q^{(0)}(x,\vartheta')\right]\left[1 - \cos(\vartheta - \vartheta')\right] d\vartheta' dx'}{2\pi\sqrt{(x - x')^2 + 2\left[1 - \cos(\vartheta - \vartheta')\right]^3}} . \tag{6}$$

To do this we followed Vandrey[5] and expressed v_{n_2} and $q(x,\vartheta)$ as Fourier-series:

$$2v_{n_2} = \frac{\Gamma}{\pi}\frac{x \sin \vartheta}{x^2 + \sin^2 \vartheta} = \frac{\Gamma}{\pi}\sum_{n=0}^{\infty} \gamma_{2n+1}(x) \sin (2n+1)\vartheta \qquad (7)$$

$$q(x,\vartheta) = \frac{\Gamma}{\pi}\sum_{n=0}^{\infty} \mu_{2n+1}(x) \sin (2n+1)\vartheta \ . \qquad (8)$$

Since

$$\int_0^{2\pi} \frac{\sin (2n+1)\vartheta'\left[1 - \cos (\vartheta - \vartheta')\right]d\vartheta'}{\sqrt{(x - x')^2 + 2\left[1 - \cos (\vartheta - \vartheta')\right]^3}} =$$

$$\sin (2n+1)\vartheta \int_0^{2\pi} \frac{\cos (2n+1)\chi(1 - \cos \chi)d\chi}{\sqrt{(x - x')^2 + 2\left[1 - \cos \chi\right]^3}}$$

we obtain from equation (4) for the unknown functions $\mu_{2n+1}(x)$ the equations

$$\mu_{2n+1}(x) = \gamma_{2n+1}(x) - \int_{-\infty}^{\infty}\int_0^{2\pi} \frac{\left[\mu_{2n+1}(x') - \mu_{2n+1}(x)\right] \cos (2n+1)\chi(1 - \cos \chi)d\chi dx'}{2\pi\sqrt{(x - x')^2 + 2(1 - \cos \chi)^3}} \qquad (9)$$

and for the approximate value $\mu^{(1)}_{2n+1}(x)$

$$\mu^{(1)}_{2n+1}(x) = \gamma_{2n+1}(x) - \int_{-\infty}^{\infty}\int_0^{2\pi} \frac{\left[\gamma_{2n+1}(x') - \gamma_{2n+1}(x)\right] \cos (2n+1)\chi(1 - \cos \chi)d\chi dx'}{2\pi\sqrt{(x - x')^2 + 2(1 - \cos \chi)^3}} \ . \qquad (10)$$

The functions $\gamma_{2n+1}(x)$ have for $n = 0, 1, 2$ the values

$$\left.\begin{aligned} \gamma_1(x) &= 2x\left(1 - \frac{|x|}{\sqrt{1+x^2}}\right) \\ \gamma_3(x) &= 2x\left[1 + 4x^2 - \frac{|x|(3+4x^2)}{\sqrt{1+x^2}}\right] \\ \gamma_5(x) &= 2x\left[1 + 12x^2 + 16x^4 - \frac{|x|(5+20x^2+16x^4)}{\sqrt{1+x^2}}\right] \end{aligned}\right\} . \qquad (11)$$

For large x, $\gamma_{2n+1}(x)$ behaves as $\frac{2}{(2x)^{2n+1}}$.

We have determined numerically some values of the integral in equation (10) and have plotted the resulting values of $\mu^{(1)}_{2n+1}(x)$ in Fig.2 together with the values of $\gamma_{2n+1}(x) = \mu^{(0)}_{2n+1}(x)$.

We note from Fig.2 that the differences between $\mu^{(1)}_{2n+1}(x)$ and $\mu^{(0)}_{2n+1}(x)$ are not very large. The ratio

$$\frac{\Delta^{(1)}\mu_{2n+1}(x)}{\mu^{(0)}_{2n+1}(x)} = \frac{\mu^{(0)}_{2n+1}(x) - \mu^{(1)}_{2n+1}(x)}{\mu^{(0)}_{2n+1}(x)}$$

is for $n = 0$ less than 0.15, for $n = 1$ less than 0.055 and for $n = 2$ less than 0.035. The maximum value of $\frac{q^{(0)}(x,\vartheta) - q^{(1)}(x,\vartheta)}{q^{(0)}(x,\vartheta)}$ is less than 0.17. The differences $\Delta^{(1)}\mu_{2n+1}(x)$ reach their maximum value where $\mu^{(0)}_{2n+1}(x)$ has a maximum and for increasing x they tend more rapidly to zero than $\mu^{(0)}_{2n+1}(x)$, as is to be expected.

If we were to perform a second step in the iteration to determine $q(x,\vartheta)$ by calculating the integral in equation (9) with $\mu^{(1)}_{2n+1}(x)$, we can expect that $\mu^{(2)}_{2n+1}(x)$ would lie between $\mu^{(0)}_{2n+1}(x)$ and $\mu^{(1)}_{2n+1}(x)$ but noticeably closer to $\mu^{(1)}_{2n+1}(x)$. We may expect that $q^{(1)}(x,\vartheta)$ and $q^{(2)}(x,\vartheta)$ would not differ by more than about 3%.

We intend to apply the results within the framework of linear wing theory, i.e. we ignore the interference between the wing thickness and the lift.

Further we intend to calculate the downwash induced by a vortex distribution in a plane and not in the resulting cambered surface. These simplifications can involve errors of the same order as the 3% uncertainty in the source distribution $q^{(1)}(x,\vartheta)$.

We have therefore not performed any further iterations for $\mu_{2n+1}(x)$. Since the $\mu_{2n+1}(x)$ for $n > 2$ contribute less to $q(x,\vartheta)$ than the first three terms and since the relative difference $\Delta^{(1)}\mu_{2n+1}(x)/\mu^{(0)}_{2n+1}(x)$ is decreasing with increasing n , we have not calculated $\Delta^{(1)}\mu_{2n+1}(x)$ for $n > 2$.

We have therefore taken for the source distribution $q(x,\vartheta)$ the value

$$q(x,\vartheta) = \frac{\Gamma}{\pi}\left\{\frac{x \sin\vartheta}{x^2 + \sin^2\vartheta} - \Delta^{(1)}\mu_1(x) \sin\vartheta \right.$$

$$\left. - \Delta^{(1)}\mu_3(x) \sin 3\vartheta - \Delta^{(1)}\mu_5(x) \sin 5\vartheta \right\} . \qquad (12)$$

We quote in Table 1 some values of the functions $\Delta^{(1)}\mu_1$, $\Delta^{(1)}\mu_3$, $\Delta^{(1)}\mu_5$ in case someone might want to calculate for example the streamwise velocities induced at the body surface.

2.3 Downwash in the plane through the vortex and the axis of the fuselage

We consider now the velocities which the source distribution $q(x,\vartheta)$ on the fuselage induces in the plane $z = 0$, i.e. the plane through the vortex and the axis of the fuselage.

If we consider a pair of source elements at x, ϑ and $x, -\vartheta$ and remember that the strength of these elements is the same but of opposite sign, then we find that in the plane of symmetry $\vartheta = 0$ such a pair does not produce a velocity component v_x nor a component v_y , but only a component v_z . From this follows that the total source distribution on the fuselage does not produce v_x or v_y velocities in the plane $z = 0$.

The source distribution $q(x,\vartheta)$ produces in $z = 0$ the additional downwash

$$-\Delta v_z(x,y,0) = \int_{-\infty}^{\infty}\int_{0}^{2\pi} \frac{q(x',\vartheta)}{4\pi} \frac{\sin\vartheta \, d\vartheta dx'}{\sqrt{(x - x')^2 + (y - \cos\vartheta)^2 + \sin^2\vartheta}^3}$$

$$= \int_{-\infty}^{\infty}\int_{0}^{2\pi} \frac{q(x',\vartheta)}{4\pi} \frac{\sin\vartheta \, d\vartheta dx'}{\sqrt{(x - x')^2 + y^2 + 1 - 2y\cos\vartheta}^3} .$$

(Note that a positive v_z velocity is directed upwards.) This equation can be written in the form

$$- \Delta v_z(x,y,0) = \int_{-\infty}^{\infty} \int_0^{2\pi} \frac{[q(x',\vartheta) - q(x,\vartheta)] \sin\vartheta \, d\vartheta dx'}{4\pi \sqrt{(x - x')^2 + y^2 + 1 - 2y\cos\vartheta}^3} + \int_0^{2\pi} \frac{q(x,\vartheta) \sin\vartheta \, d\vartheta}{2\pi[y^2 + 1 - 2y\cos\vartheta]} \quad . \tag{13}$$

The single integral gives the $-\Delta v_z(x,y,0)$ produced by a distribution of two-dimensional source lines $q(\vartheta,x)$ on the circle $y^2 + z^2 = 1$.

The integral

$$- \Delta v_z^{(0)}(x,y,0) = \int_0^{2\pi} \frac{q^{(0)}(x,\vartheta) \sin\vartheta \, d\vartheta}{2\pi[y^2 + 1 - 2y\cos\vartheta]} \tag{14}$$

may be called the approximation from slender theory, where we would assume that $v_{n_1}(x,\vartheta)$ and $q(x,\vartheta)$ vary only slowly with x .

With $q^{(0)}(x,\vartheta) = \frac{\Gamma}{\pi} \frac{x \sin\vartheta}{x^2 + \sin^2\vartheta}$ we obtain:

$$\begin{aligned}
- \Delta v_z^{(0)}(x,y,0) &= \frac{2\Gamma}{\pi^2} \int_0^{\pi/2} \frac{x \sin^2\vartheta \, (1+y^2) d\vartheta}{[x^2 + \sin^2\vartheta][(y^2+1)^2 - 4y^2\cos^2\vartheta]} \\
&= \frac{2\Gamma}{\pi^2} \int_0^{\pi/2} \frac{x(1+y^2) \sin^2\vartheta \, d\vartheta}{[x^2 + \sin^2\vartheta][(y^2-1)^2 + 4y^2\sin^2\vartheta]} \\
&= \frac{2\Gamma}{\pi^2} \frac{(y^2+1)}{[4y^2x^2 - (y^2-1)^2]} \int_0^{\pi/2} \left\{ \frac{x^3}{x^2 + \sin^2\vartheta} - \frac{(y^2-1)^2}{4y^2} \frac{x}{\left[\sin^2\vartheta + \frac{(y^2-1)^2}{4y^2}\right]} \right\} d\vartheta \\
&= \frac{\Gamma}{\pi} \frac{(y^2+1)}{[4y^2x^2 - (y^2-1)^2]} \left\{ \frac{x^3}{|x|\sqrt{1+x^2}} - \frac{x(y^2-1)}{y^2+1} \right\} \quad .
\end{aligned} \tag{15}$$

In this relation we have to exclude the case $x^2 = (y^2 - 1)^2/4y^2$. For this case we obtain for $y \neq 1$

$$- \Delta v_z^{(0)}\left(x = \pm \frac{y^2 - 1}{2y}, y, 0\right) = \frac{\Gamma}{\pi} \frac{x}{|x|} \frac{y}{(y^2 + 1)^2} \quad . \tag{16}$$

With the $q(x,\vartheta)$ given in equation (12) the single integral in equation (13) has the value

$$- \Delta v_z^{(+)} = \int_0^{2\pi} \frac{q(x,\vartheta) \sin \vartheta \, d\vartheta}{2\pi[y^2 + 1 - 2y \cos \vartheta]}$$

$$= \frac{\Gamma}{\pi} \left\{ \frac{y^2 + 1}{4y^2x^2 - (y^2 - 1)^2} \left[\frac{x^3}{|x|\sqrt{1 + x^2}} - \frac{x(y^2 - 1)}{y^2 + 1} \right] \right.$$

$$\left. - \frac{1}{2y^2} \Delta^{(1)}\mu_1(x) - \frac{1}{2y^4} \Delta^{(1)}\mu_3(x) - \frac{1}{2y^6} \Delta^{(1)}\mu_5(x) \right\} \quad . \tag{17}$$

The double integral of equation (13) has been determined numerically. The value for $y = 1$, $x \to 0$ has been derived by graphical extrapolation from the values calculated for $x \neq 0$, since the author has been unable to determine analytically the limit:

$$I = \lim_{x \to 0} \int_{-\infty}^{\infty} \int_0^{2\pi} \left[\frac{x'}{x'^2 + \sin^2 \vartheta} - \frac{x}{x^2 + \sin^2 \vartheta} \right] \frac{\sin^2 \vartheta \, d\vartheta dx'}{\sqrt{(x - x')^2 + 2(1 - \cos \vartheta)^3}} \quad .$$

In Fig.3 we have plotted for the wing body junction, $y = R = 1$, the chordwise distribution of the additional downwash, $-\Delta v_z$, produced by the source distribution on the fuselage, together with the downwash induced by the vortex line itself: $\frac{-1}{2\pi x/R}$. The curve Δv_z is obtained from equation (13); $\Delta v_z^{(0)}$ is the result from slender theory, equations (14) to (16); and $\Delta v_z^{(+)}$ is given by equation (17). The additional downwash changes its sign with x , $\Delta v_z(x) = - \Delta v_z(-x)$.

The figure shows that the interference term Δv_z cannot be neglected compared to the downwash of the isolated vortex except close to the position of

the vortex. The figure shows further that slender theory overestimates the interference close to the vortex. We note from Fig.3 and equation (15) that for large values of x, $\frac{\Delta v_z}{\Gamma/R}$ is equal to $\frac{1}{2\pi}\frac{x}{|x|}\frac{1}{\sqrt{1+x^2}}$, i.e. it is as large as the downwash produced by the vortex itself.

In Fig.4, we have plotted Δv_z and $\Delta v_z^{(0)}$ for two spanwise stations away from the junction. We note that for $y > R$, Δv_z vanishes at the position of the vortex whilst for $y = 1$, Δv_z has a discontinuity at $x = 0$, but the mean value vanishes also for $y = 1$.

This fact that the interference between a straight vortex and a fuselage with fore and aft symmetry vanishes at the position of the vortex has been noted by Lennertz[6] and Vandrey[5]. Within the framework of the so-called 'lifting line' theory this fact has been interpreted as implying that there is no interference between an unswept plane wing of infinite aspect ratio at an angle of incidence and a cylindrical fuselage in midwing position at zero angle of incidence. In the next sections we shall demonstrate that this interpretation gives misleading results.

The Δv_z values given in Fig.4 show that the body effect decreases rapidly with distance from the junction. For large x it decreases as $(R/y)^2$, i.e. as in two-dimensional flow, or in slender theory. For small x, the interference effect decreases more rapidly.

3 DESIGN OF THE CAMBER SURFACE OF A WING-FUSELAGE COMBINATION FOR A GIVEN CHORDWISE LOAD DISTRIBUTION

We consider now an unswept wing of constant chord, c, and infinite aspect ratio, attached to a circular fuselage in the midwing position. The wing is supposed to have a camber surface $z_s(x,y)$ such that the load distribution $-\Delta C_p(x,y)$ is constant along the span. For a thin wing $-\Delta C_p(x,y) = 2\gamma(x,y) = 2\gamma(x)$.

The required camber surface can be calculated by means of the downwash for a single straight vortex, if we make the approximations of linear theory and assume the vortices to lie in the chordal plane and approximate the normal velocity at the camber surface by the downwash induced in the chordal plane.

We obtain for the camber surface $z_s(x,y)$ the equation

$$\frac{\partial z_s(x,y)}{\partial x} = \frac{v_z(x,y,z=0)}{V_0}$$

$$= \int_0^{c/R} \frac{\gamma(x')}{V_0} \left[\frac{-1}{2\pi\left(\frac{x}{R} - \frac{x'}{R}\right)} + \frac{\Delta v_z\left(\frac{x}{R} - \frac{x'}{R}\,;\, y\,;\, z=0\right)}{\Gamma/R} \right] d\left(\frac{x'}{R}\right) \qquad (18)$$

with $\Delta v_z\left(\frac{x}{R},y,0\right)$ from equation (13) or from Figs.3 and 4.

As a first example we have chosen the load distribution

$$\gamma(x) = 2\alpha V_0 \sqrt{\frac{c-x}{x}}\,, \qquad 0 < x < c \qquad (19)$$

which gives for the isolated wing a flat plate, $\partial z_s(x,y)/\partial x = -\alpha$.

Fig.5 shows the slope of the camber surface in the wing-body junction and the shape of the section. We note that a positive twist and some positive camber is required for the section in the junction. The figure shows that the interference effect is quite large in the junction, except for fuselages where the body radius is large compared to the wing chord, i.e. the case where the fuselage acts as a plane normal to the plane of the wing.

Fig.6 shows the slope of the wing, also in the wing-body junction, for the load distributions given by the second and the third term of the Birnbaum series.

Fig.7 gives the slope of the wing for the flat plate load distribution, equation (19), and $R/c = 0.2$, at a few spanwise stations away from the junction. To judge the importance of the interference effect for fuselages of different size, it seems more relevant to measure the spanwise distance with respect to the wing chord. We have noted in Fig.4 that the interference downwash Δv_z of a single vortex decreases with distance from the junction at least as $(R/y)^2$. The interference effect decreases therefore more rapidly for bodies with smaller R/c , but the effect in the junction is larger for smaller bodies.

In Fig.8 we compare the slope in the junction calculated with the interference term from slender theory $\Delta v_z^{(0)}$, see Fig.3 and equation (15), with the slope calculated with Δv_z , equation (13). We note that slender theory gives

a qualitatively correct estimate of the interference effect; the numerical values are for the chosen example about 20% too large. The percentage error increases of course with decreasing c/R ; it is about 60% for $c/R = 1$.

4 THE LOAD DISTRIBUTION OF A GIVEN WING ATTACHED TO A FUSELAGE AT ZERO ANGLE OF INCIDENCE IN MIDWING POSITION

In practice, one is just as much, if not more so, interested in the problem of determining the load distribution for a given wing at a given angle of incidence in the presence of a fuselage. With the isolated wing, the solution of this problem requires already far more numerical work than the design problem, since an integral equation has to be solved.

If one were to attempt a solution of the wing-fuselage problem by an iteration procedure, then it would be necessary to determine for each modification to the load distribution of the wing the modification to the source distribution on the fuselage and its effect on the downwash at the wing. To solve the problem in this way would be very laborious. One would probably prefer to obtain an approximate solution, in a manner similar to that of Ref.7, by means of panels of constant source distribution on the surface of the configuration and panels of constant doublet strength on the camber surface and in the wake. We have seen in Fig.7 that the body effect can vary rapidly along the span. This makes it necessary to use a large number of panels if one wants to be able to extrapolate to the load distribution in the junction.

We intend in this section to make use of the results obtained so far, to derive some modification to the existing approximate methods for determining the load distribution on wing-fuselage combinations, which are based on the work of Küchemann[1] and Multhopp[2,3].

To do so, we want first to interpret some implications of the wing-body interference in a manner somewhat different from the previous section. We ask, what is the load distribution of a wing with a given shape at the junction, if the remainder of the wing has a shape such that the load distribution is constant along the span? (We note that this is not a problem which arises in practice.)

To answer this question, we have to find a solution of equation (18), for the special case $y = R$, with $\partial z_s/\partial x$ given. We consider the special case that in the junction the wing has an uncambered section at the angle of incidence α . As stated above, we are only working to the accuracy of linear theory,

i.e. we are dealing with the limit $\alpha \to 0$. This means that the variation of the wing height with respect to the axis of the fuselage is ignored.

Equation (18) cannot be inverted analytically, as without the interference term. We have therefore determined only a crude approximation to the load distribution by expressing $\gamma(x)$ as a sum of the first three terms in the Birnbaum series. For $R/c = 0.2$, an approximately flat section is obtained from

$$\gamma(x) = 1.5\sqrt{\frac{1 - x/c}{x/c}} - \sqrt{\frac{x}{c}\left(1 - \frac{x}{c}\right)} - \left(1 - 2\frac{x}{c}\right)\sqrt{\frac{x}{c}\left(1 - \frac{x}{c}\right)} \quad . \qquad (20)$$

The slope of the section and the load distribution are plotted in Fig.9.

The most important fact is that the lift coefficient is 37% smaller than for a wing without fuselage, which has the same section throughout as the wing-fuselage combination has in the junction. We must however remember that for the wing-fuselage combination considered the section varies along the span.

In practice, we are more interested in wing-body combinations, where the wing has the same flat section along the span. For this the load distribution varies along the span and the lift coefficient further outboard tends to $2\pi\alpha$. The ensuing system of trailing vortices is such that it produces an upwash in the junction which means the lift there is larger for the flat wing than for the cambered wing with the flat junction.

To obtain an estimate of the C_L-distribution of the flat wing at incidence in the presence of the fuselage at zero incidence, we make use of the concepts of Küchemann's method[1] for calculating the spanwise loading on isolated wings. There, the chordwise load distribution is expressed as the sum of two terms. The first is the load distribution of the corresponding two-dimensional section; this distribution is derived by ignoring the spanwise variation of the load distribution, i.e. the trailing vortices are ignored. For the wing-fuselage combination, the corresponding term $-\Delta C_p(x;y) = 2\gamma(x;y)$ is the solution of equation (18). The effect of the trailing vortices is approximated by a downwash $\alpha_i(y)$, which is constant along the chord, i.e. the second term in the load distribution is $\alpha_i \Delta C_p(x,y;\ \alpha = 1)$.

To determine the downwash induced by the wing trailing vortices in the presence of the fuselage, we apply the method developed by Multhopp[2] and extended in Ref.3. The equation to be solved, equation (16) of Ref.3, differs from the one used previously in that we take for the sectional lift slope,

$a = C_L/\alpha_{eff}$, at the junction a value which differs from that of the isolated straight wing.

The spanwise variation of the lift slope, $a(y)$, can be determined from equation (18), by calculating for various $y > R$ and given R/c and $\frac{\partial z_s(x;y)}{\partial x} = -\alpha$ the load distribution $\gamma(x;y)$ and

$$a(y) = 2 \int_0^1 \frac{\gamma(x;y)}{\alpha} d\left(\frac{x}{c}\right) .$$

We have not done such calculations, but have approximated $a(y)$ by the relation

$$a(y) = a_J \left(\frac{R}{y}\right)^2 + 2\pi \left[1 - \left(\frac{R}{y}\right)^2\right] , \qquad (21)$$

similar to the spanwise variation of Δv_z , see Fig.4. The accuracy of this approximation is consistent with the accuracy of the Küchemann method.

In Fig.10, we show the effect of the variable $a(y)$ on the spanwise C_L distribution for the example of an unswept tapered wing with aspect ratio $A = 6$, for which the ratio between the body diameter and the wing span is 0.1 and the ratio between the body radius and the wing chord at the centre section is 0.2. We note a considerable reduction of the lift near the junction.

We also know from Figs.5 and 6 that the difference $2\pi - a_J$ is reduced when the ratio R/c increases. We have determined some approximate values of a_J as a function of R/c in the same way as above, using again only the first three terms of the Birnbaum series for $\gamma(x)$. The result is plotted in Fig.11. We shall at a later date solve equation (18) to a higher accuracy.

The chordwise load distribution in the junction, plotted in Fig.9, differs from that of the isolated wing in one further respect, namely in that its centre of pressure is further forward. For the example plotted, $x_{cp}/c = 0.225$, compared to $x_{ac}/c = 0.25$ for the isolated wing. If more terms of the Birnbaum series for $\gamma(x;y = R)$ had been used to obtain a better approximation to $\partial z_s(x,y = R)/\partial x = -\alpha$, then x_{cp} would be somewhat forward of 0.225c. Within the framework of Küchemann's method, the chordwise load distribution at the junction of the uncambered wing at angle of incidence attached to the fuselage at zero incidence would also be approximated by the one given in Fig.9 (or by equation (20)) except for the factor $1 - \frac{\alpha_{i\ \text{junction}}}{\alpha}$.

5 FURTHER WORK

Except for part of the last section, we have considered only wings of constant chord, infinite aspect ratio and constant spanwise load distribution.

Küchemann's framework can be used to design swept wings of finite aspect ratio for a given load distribution and to determine the load distribution of given wings. His method is based on a relation for the downwash induced by the bound vortices which was derived from wings of infinite aspect ratio and spanwise constant load distributions.

With straight wings attached to a fuselage at zero incidence, the corresponding relation is given by equation (18). We can therefore in a similar manner derive approximate methods for designing wing-fuselage combinations with wings of finite aspect ratio and given load distribution.

For the isolated wing, Küchemann has simplified the task by a further modification to the relation for the downwash. He has approximated it by an equation which can be inverted analytically, so that for a given chordwise distribution of the downwash the strength of the bound vortices can be calculated from an integral over the downwash. We have not yet obtained an approximation to equation (18) which can be inverted analytically, so that we still need to solve an integral equation numerically. The function $\Delta v_z\left(\frac{x}{R},y\right)$ in equation (18) can of course be approximated by analytic expressions as, for example, for $y/R = 1$ and $\left|\frac{x}{R}\right| < 5$:

$$\frac{\Delta v_z}{\Gamma/R} = \frac{x}{|x|}\, 0.105 \left[1 - 0.4\,\frac{|x|}{1+|x|} - 0.1\left(\frac{x}{1+|x|}\right)^2 - 0.5\left(\frac{|x|}{1+|x|}\right)^3\right] .$$

The design of an isolated wing can of course be improved by dealing with the complete equation for the downwash related to a given load distribution of a finite aspect ratio wing. Similarly, the design of a wing-body combination can be improved by calculating the normal velocity at the fuselage which is induced by the bound and the trailing vortices related to a given load distribution.

Before starting with this problem, it is planned to consider the combination of a cylindrical fuselage with a swept wing. For this the design problem is of practical interest, e.g. with respect to transport aircraft designed for high subsonic cruise, see, for example, Ref.8. We shall again consider wings of constant chord and infinite aspect ratio with a given chordwise load

distribution which is constant along span and derive a relation between the downwash and the bound vortices.

Further, fuselages in off-centre position have to be considered. With these an uncambered untwisted wing of finite thickness produces a lift at zero wing incidence. We shall therefore also deal with the thickness problem. In preparation for this, we intend to begin again with an unswept wing of infinite aspect ratio in midwing position.

6 CONCLUSIONS

The flow field past a single straight vortex crossing a cylindrical circular fuselage at right angles has been studied, in particular the downwash induced in the plane containing the vortex and the axis of the fuselage has been determined numerically.

From this the shape of a wing-body combination with an unswept wing of infinite aspect ratio has been found, for which the chordwise load distribution is given and the load is constant along the span. The results show that it is wrong to assume that a cylindrical fuselage at zero incidence does not affect the chordwise or spanwise load distribution of an unswept wing of infinite aspect ratio and constant shape along the span.

If the framework of Küchemann's method[1] for calculating the load distribution on isolated wings is used, then it is possible to take account of the interference effect on the chordwise load distribution and modify the method of Ref.3 for calculating the load distribution on wing-fuselage combinations.

Acknowledgment

The author is indebted to Mrs. M.G. Joyce for having written all the computer programmes related to the numerical work referred to in this paper.

Table 1

VALUES OF FOURIER COEFFICIENTS IN EQUATION (12)

x/R	$\Delta^{(1)}\mu_1$	$\Delta^{(1)}\mu_3$	$\Delta^{(1)}\mu_5$
0.05	0.0121	0.0045	0.0027
0.1	0.0226	0.0075	0.0040
0.15	0.0324	0.0095	0.0044
0.2	0.0423	0.0113	0.0046
0.3	0.0587	0.0125	0.0038
0.4	0.0710	0.0117	0.0025
0.5	0.0798	0.0100	0.0013
0.6	0.0852	0.0078	0.0005
0.8	0.0883	0.0039	0
1.0	0.0843	0.0013	
1.5	0.0620	0	
2	0.0399		
2.5	0.0240		
3	0.0139		
4	0.0040		
5	0.0005		

SYMBOLS

A	aspect ratio
$a(y)$	sectional lift slope
a_J	sectional lift slope in wing-body junction
b	wing span
c	wing chord
C_L	lift coefficient
C_p	pressure coefficient
ΔC_p	difference between pressure coefficients on upper and lower surface
$q(x,\vartheta)$	strength of source distribution
R	radius of fuselage
x,y,z	rectangular coordinate system, x along the axis of the fuselage
x,r,ϑ	system of cylinder coordinates
V_0	free stream velocity
v_x,v_y,v_z	velocity components
Δv_z	interference velocity for a single vortex (induced by the source distribution on the fuselage)
$\Delta v_z^{(0)}$	interference velocity according to slender theory
v_n	velocity component normal to the surface of the fuselage
$z_s(x,y)$	ordinate of the mean surface of the wing
α	geometric angle of incidence
α_{eff}	effective angle of incidence
Γ	vortex strength of single vortex
$\gamma(x)$	local strength of vortex distribution
γ_{2n+1}	Fourier coefficients defined by equation (7)
μ_{2n+1}	Fourier coefficients defined by equation (8)
φ	angle of sweep

REFERENCES

No.	Author	Title, etc.
1	D. Küchemann	A simple method for calculating the span and chordwise loading on straight and swept wings of any given aspect ratio at subsonic speeds. ARC R & M 2935 (1952)
2	H. Multhopp	Aerodynamics of the fuselage. Luftfahrtforsch, 18, 52 (1941) RTP Transl. 1220, ARC 5263
3	J. Weber D.A. Kirby D.J. Kettle	An extension of Multhopp's method of calculating the spanwise loading of wing-fuselage combinations. ARC R & M 2872 (1951)
4	J.L. Hess A.M.O. Smith	Calculation of potential flow about arbitrary bodies. Progress in Aeron. Scs., Vol. 8, 1 (1967)
5	F. Vandrey	Zur theoretischen Behandlung des gegenseitigen Einflusses von Tragflügel und Rumpf. Luftfahrtforsch, 14, 347 (1937)
6	J. Lennertz	Beitrag zur theoretischen Behandlung des gegenseitigen Einflusses von Tragfläche und Rumpf. Z. angew. Math. Mech. 7, 17 (1927)
7	P.E. Rubbert G.R. Saaris	A general three-dimensional potential-flow method applied to V/STOL aerodynamics. SAE 680304 (1968)
8	J.A. Bagley	Some aerodynamic principles for the design of swept wings. Prog. Aeron. Scs., 3, 1 (1962)

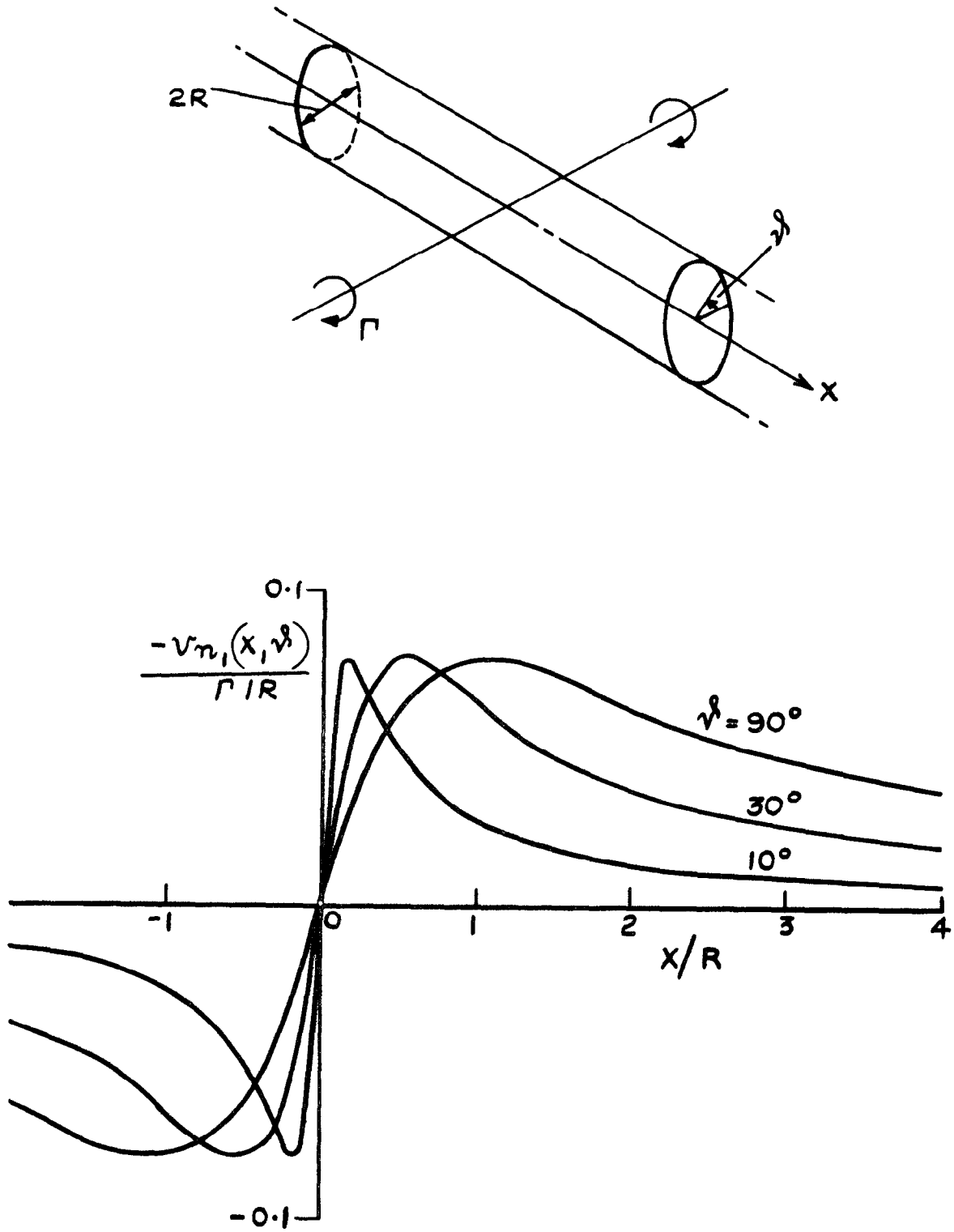

Fig.1 Normal velocities at the fuselage induced by a straight vortex

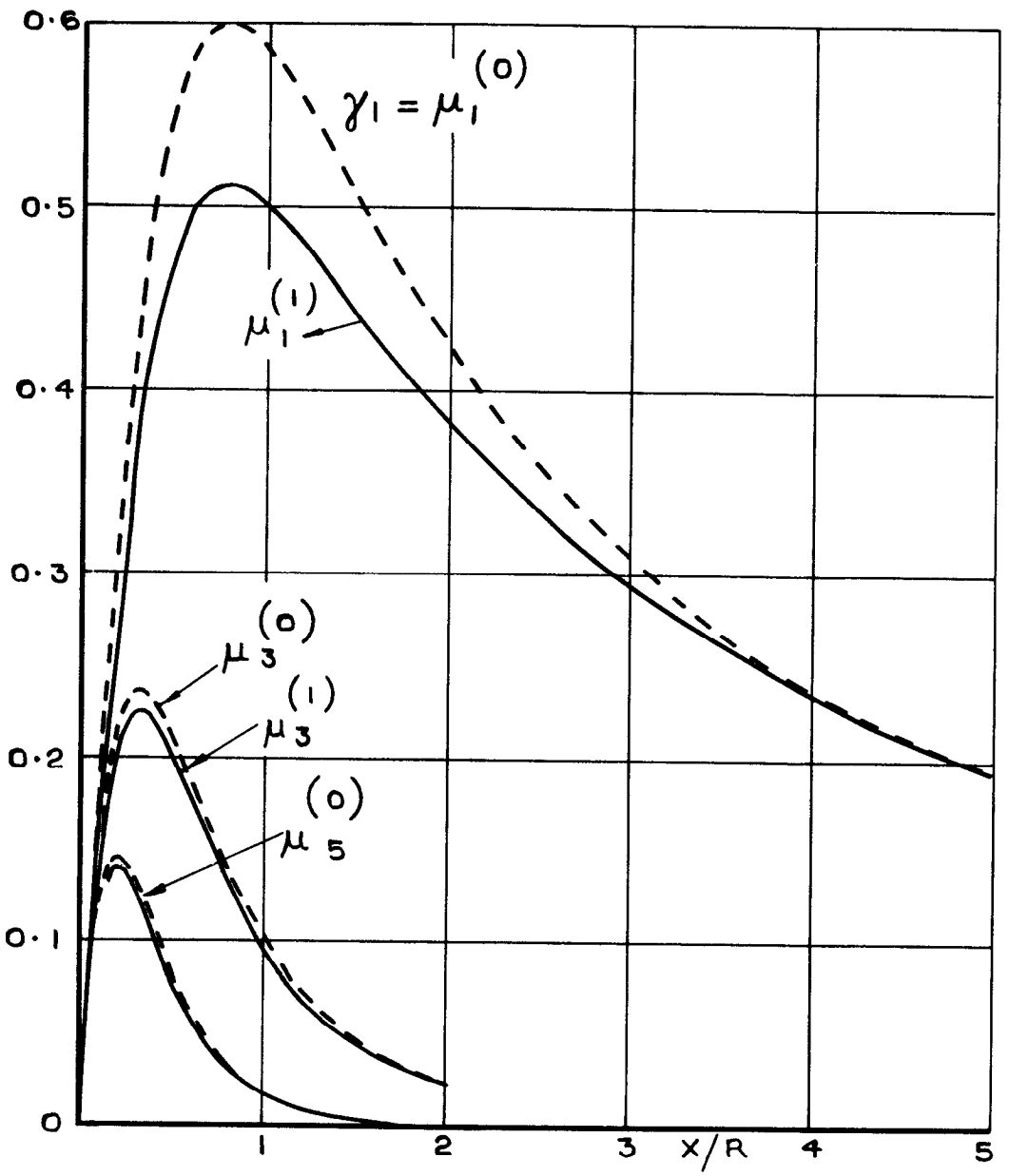

Fig. 2 Approximate values of the Fourier coefficients for the source distribution on the fuselage, see eqn (8)

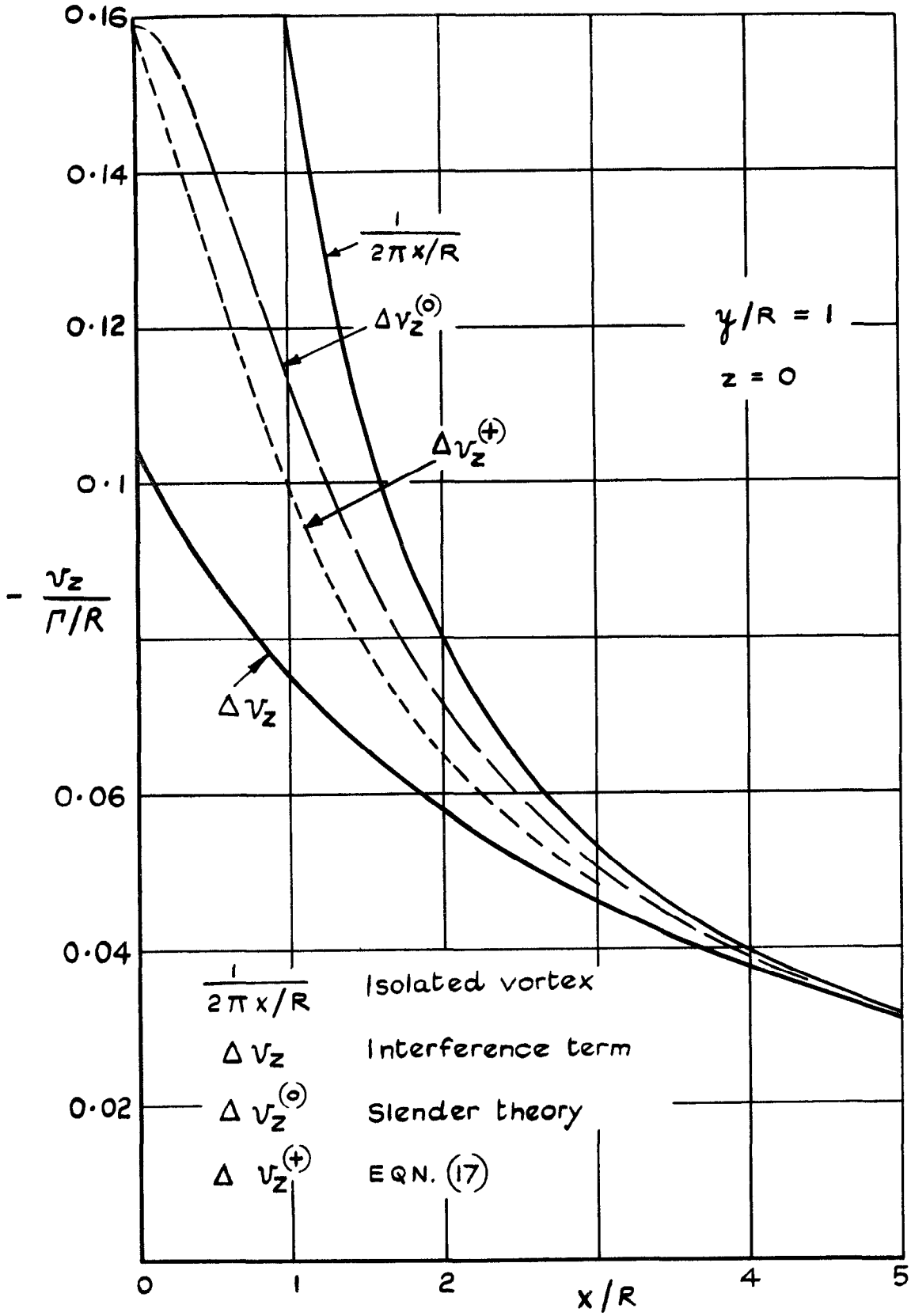

Fig. 3 Various downwash contributions in the wing-body junction induced by a single vortex in X=O

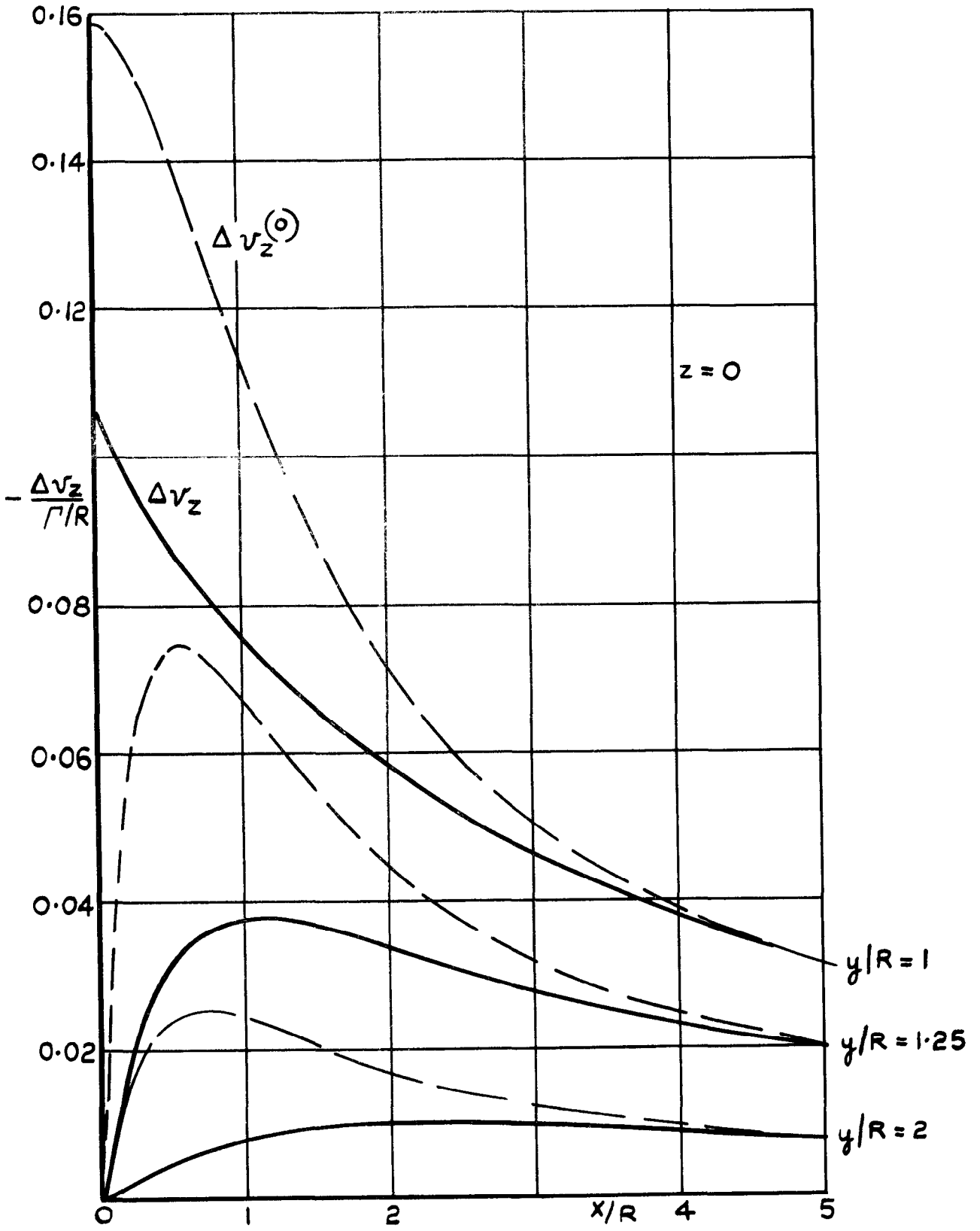

Fig. 4 Additional downwash at various spanwise stations

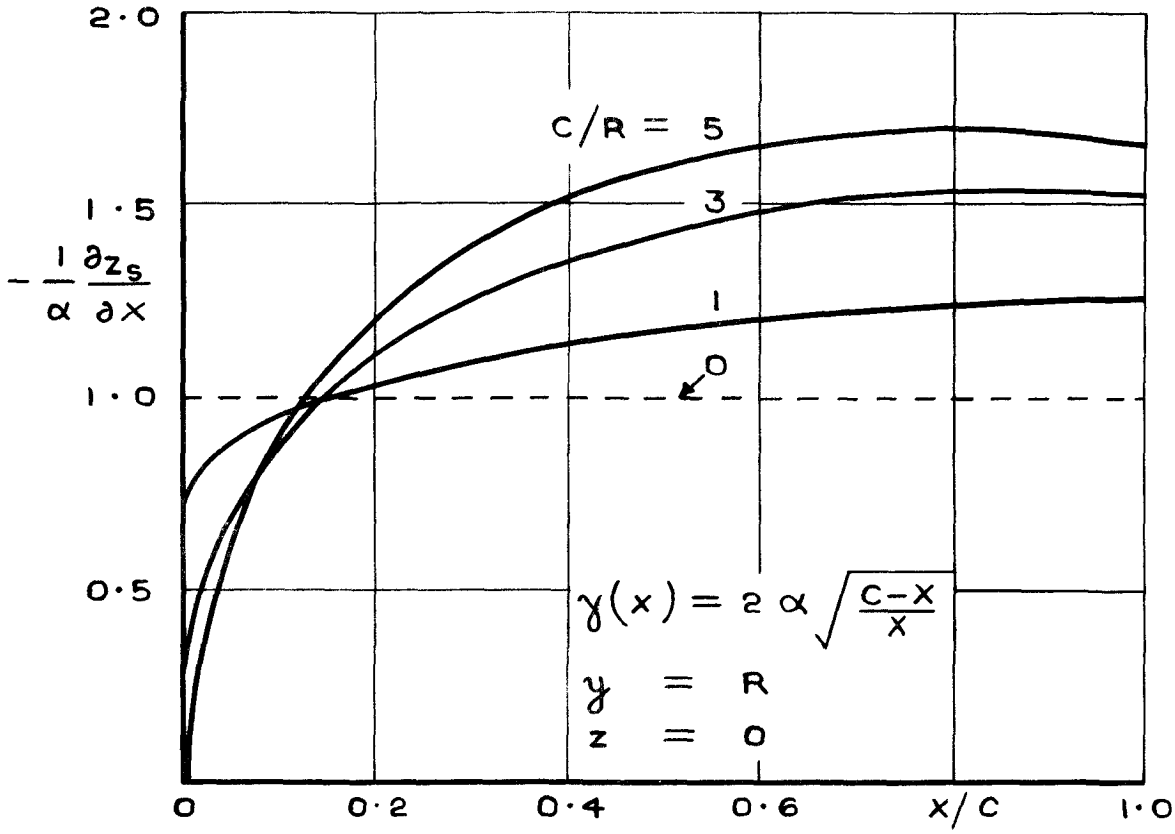

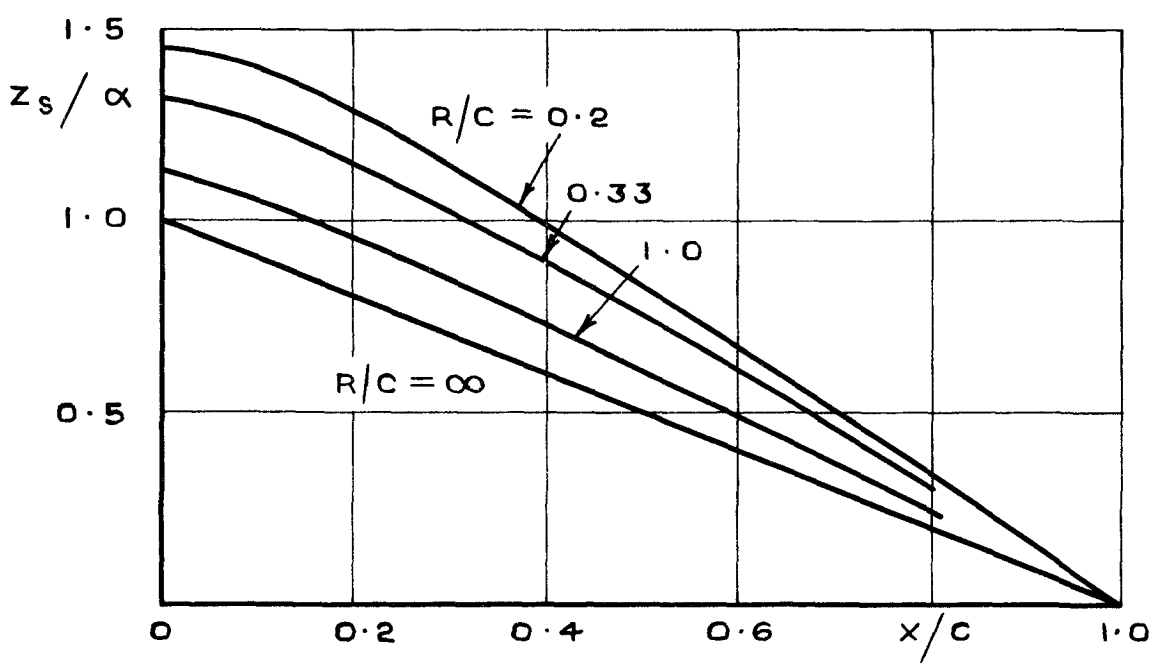

Fig. 5 Section shape in the wing – body junction

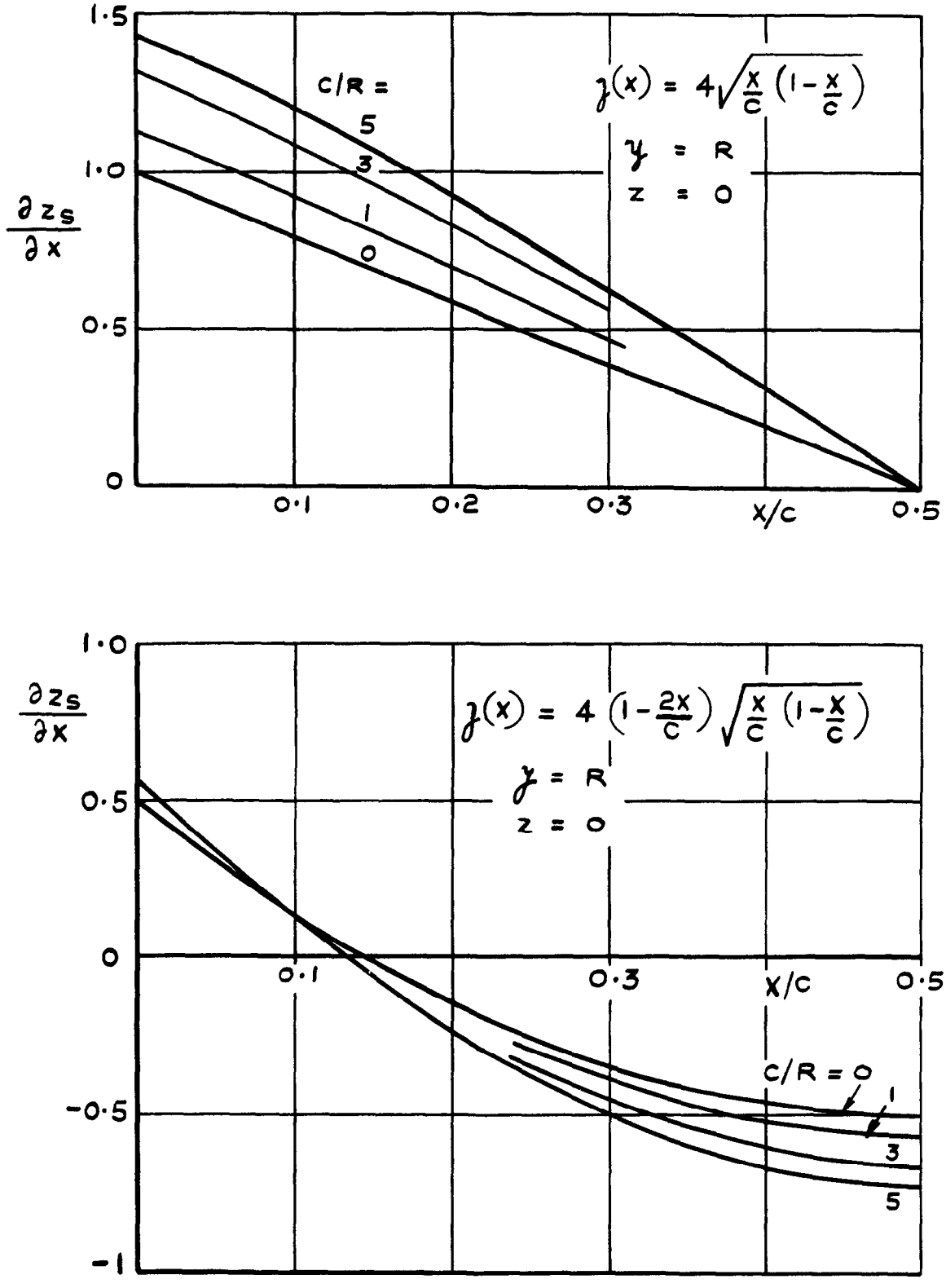

Fig. 6 Section shape in the wing-body junction

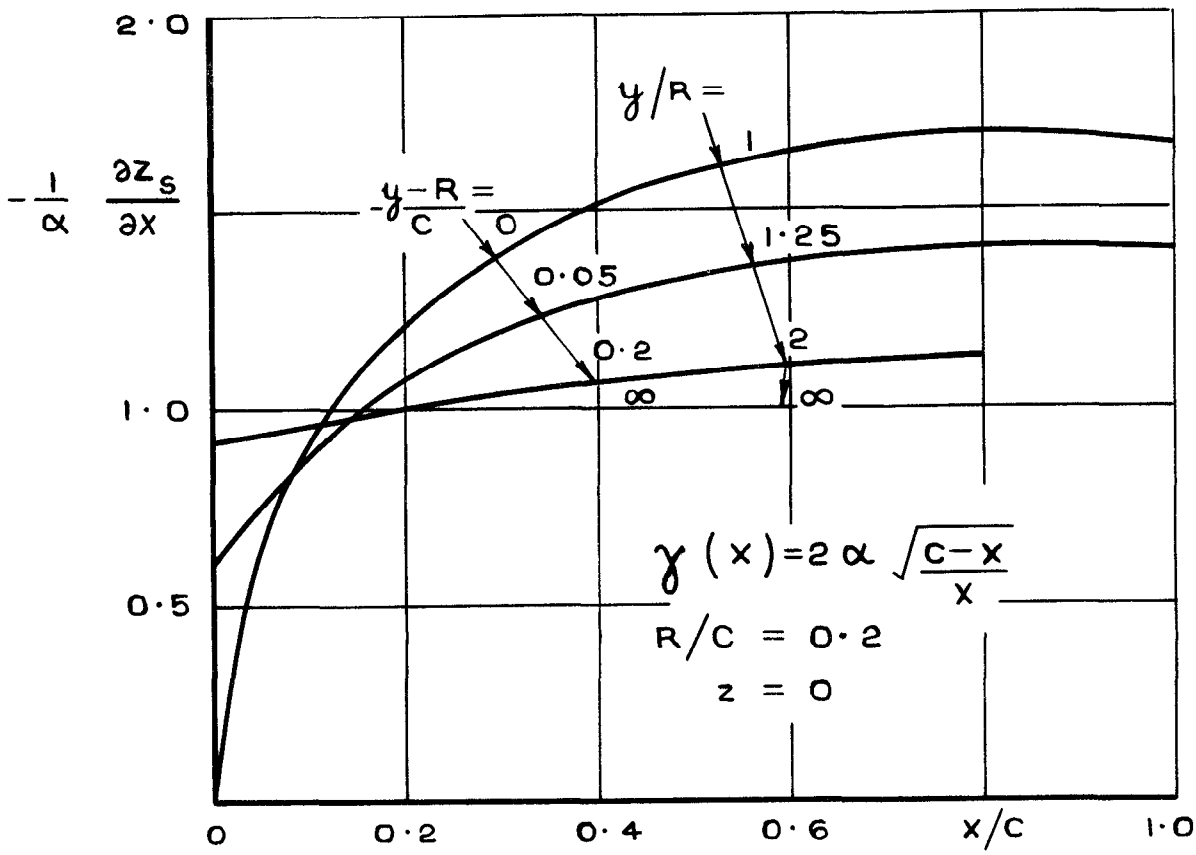

Fig.7 Slope of chordwise sections

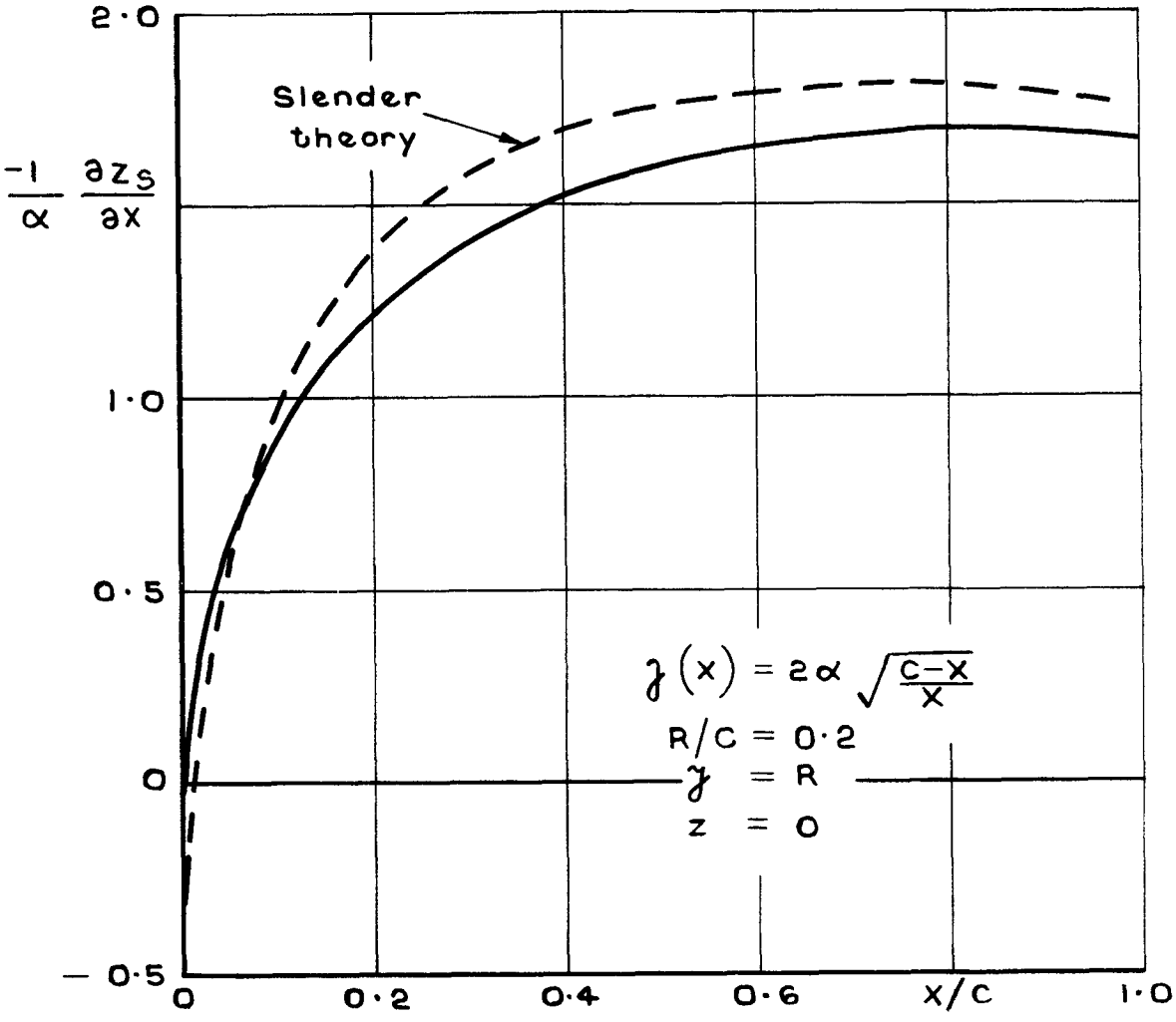

Fig. 8 Slope of section in wing-body junction

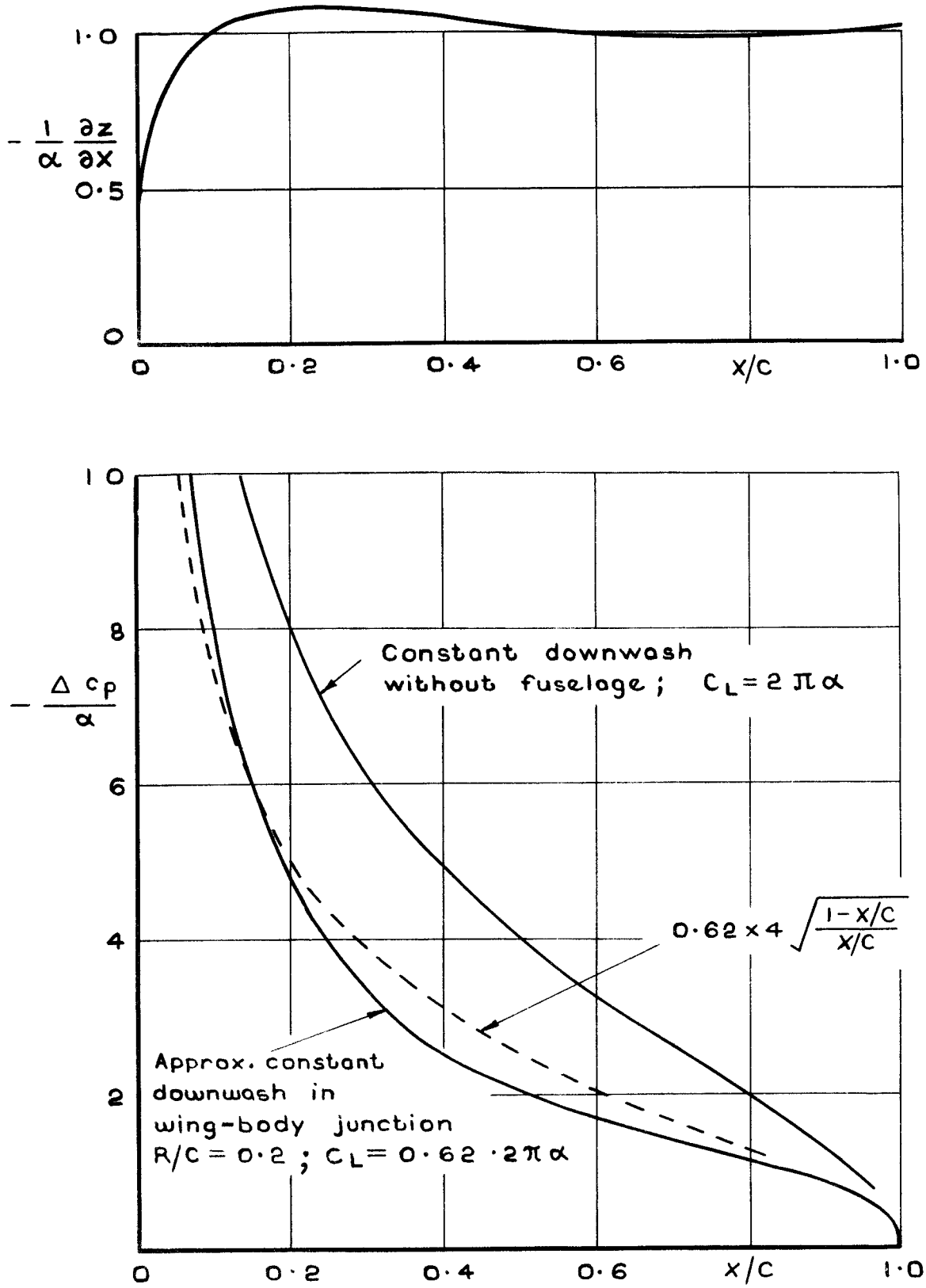

Fig. 9 Load distribution for uncambered section at incidence

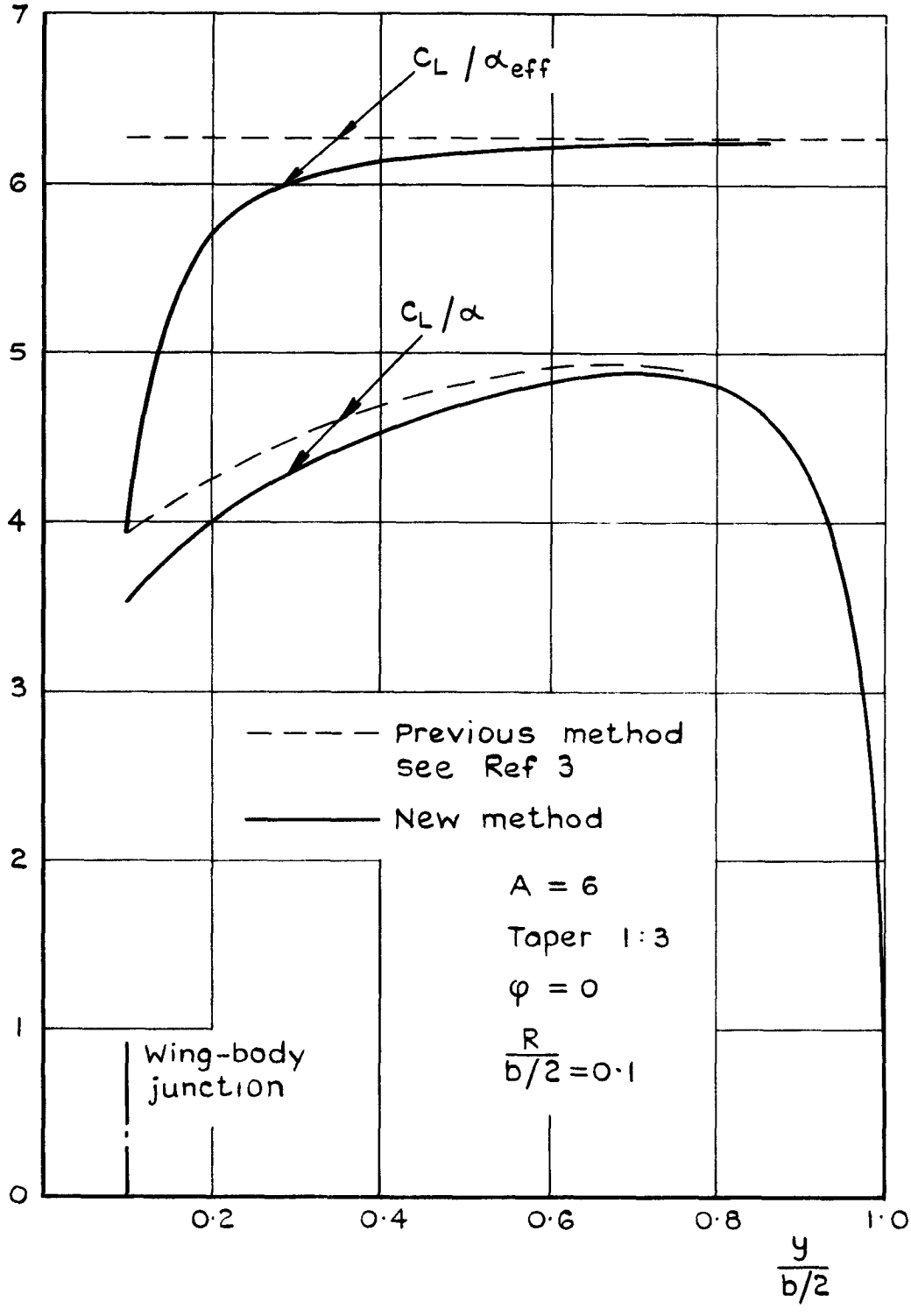

Fig.10 Effect of sectional lift slope on spanwise C_L distribution

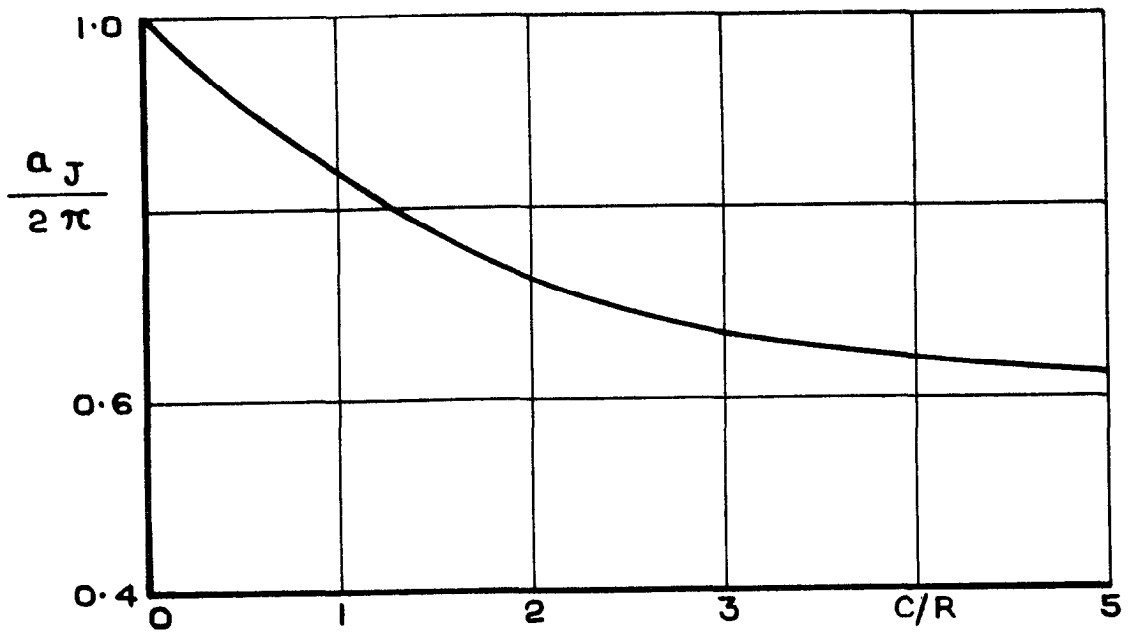

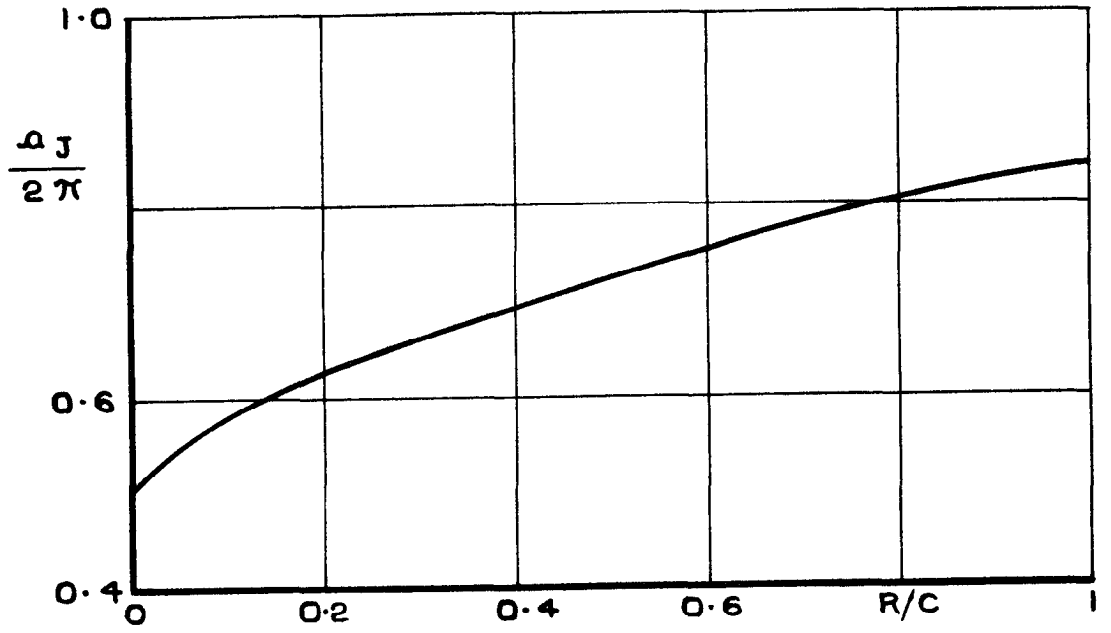

Fig.11 Sectional liftslope in the wing–body junction

Printed in England for Her Majesty's Stationery Office by the Royal Aircraft Establishment, Farnborough Dd. 289030 K5 10/75

ARC CP No.1331
July 1969

Weber, J.

INTERFERENCE PROBLEMS ON WING-FUSELAGE COMBINATIONS. PART I: LIFTING UNSWEPT WING ATTACHED TO A CYLINDRICAL FUSELAGE AT ZERO INCIDENCE IN MIDWING POSITION

533.695.12 :
533.693.2
533.696.3 :
533.6.011.32 :
533.6.048.3 :
533.6.041 :
518.1

The incompressible flow field past a single straight vortex line which crosses a cylindrical circular fuselage at right angles has been studied. In particular the downwash induced in the plane through the vortex and the axis of the fuselage has been determined numerically.

The results are used to solve the design problem for an unswept wing of infinite aspect ratio for which the chordwise load distribution is given and the spanwise distribution in the presence of the fuselage is required to be constant. It is shown how the interference effect varies with the ratio R/c between the body radius and the wing chord, and with the spanwise distance from the junction.

A modification of existing methods for calculating the spanwise load distribution of wing-fuselage combinations is suggested to take account of the body interference with the chordwise load distribution.

ARC CP No.1331
July 1969

Weber, J.

INTERFERENCE PROBLEMS ON WING-FUSELAGE COMBINATIONS. PART I LIFTING UNSWEPT WING ATTACHED TO A CYLINDRICAL FUSELAGE AT ZERO INCIDENCE IN MIDWING POSITION

533.695.12 .
533.693.2 .
533.696.3 :
533.6.011.32 :
533.6.048.3
533.6.041 :
518.1

The incompressible flow field past a single straight vortex line which crosses a cylindrical circular fuselage at right angles has been studied. In particular the downwash induced in the plane through the vortex and the axis of the fuselage has been determined numerically.

The results are used to solve the design problem for an unswept wing of infinite aspect ratio for which the chordwise load distribution is given and the spanwise distribution in the presence of the fuselage is required to be constant. It is shown how the interference effect varies with the ratio R/c between the body radius and the wing chord, and with the spanwise distance from the junction.

A modification of existing methods for calculating the spanwise load distribution of wing-fuselage combinations is suggested to take account of the body interference with the chordwise load distribution.

Cut here

ARC CP No.1331
July 1969

Weber, J.

INTERFERENCE PROBLEMS ON WING-FUSELAGE COMBINATIONS. PART I: LIFTING UNSWEPT WING ATTACHED TO A CYLINDRICAL FUSELAGE AT ZERO INCIDENCE IN MIDWING POSITION

533.695.12 :
533.693.2 .
533.696.3 :
533.6.011.32 :
533.6.048.3 ·
533.6.041 :
518.1

The incompressible flow field past a single straight vortex line which crosses a cylindrical circular fuselage at right angles has been studied. In particular the downwash induced in the plane through the vortex and the axis of the fuselage has been determined numerically.

The results are used to solve the design problem for an unswept wing of infinite aspect ratio for which the chordwise load distribution is given and the spanwise distribution in the presence of the fuselage is required to be constant. It is shown how the interference effect varies with the ratio R/c between the body radius and the wing chord, and with the spanwise distance from the junction.

A modification of existing methods for calculating the spanwise load distribution of wing-fuselage combinations is suggested to take account of the body interference with the chordwise load distribution.

Cut here

ARC CP No.1331
July 1969

Weber, J.

INTERFERENCE PROBLEMS ON WING-FUSELAGE COMBINATIONS. PART I: LIFTING UNSWEPT WING ATTACHED TO A CYLINDRICAL FUSELAGE AT ZERO INCIDENCE IN MIDWING POSITION

533.695.12 :
533.693.2 :
533.696.3 :
533.6.011.32 ·
533.6.048.3 :
533.6.041 ·
518.1

The incompressible flow field past a single straight vortex line which crosses a cylindrical circular fuselage at right angles has been studied. In particular the downwash induced in the plane through the vortex and the axis of the fuselage has been determined numerically.

The results are used to solve the design problem for an unswept wing of infinite aspect ratio for which the chordwise load distribution is given and the spanwise distribution in the presence of the fuselage is required to be constant. It is shown how the interference effect varies with the ratio R/c between the body radius and the wing chord, and with the spanwise distance from the junction.

A modification of existing methods for calculating the spanwise load distribution of wing-fuselage combinations is suggested to take account of the body interference with the chordwise load distribution.

Cut here

DETACHABLE ABSTRACT CARDS

DETACHABLE ABSTRACT CARDS

1975

Published by
HER MAJESTY'S STATIONERY OFFICE

Government Bookshops
49 High Holborn, London WC1V 6HB
13a Castle Street, Edinburgh EH2 3AR
41 The Hayes, Cardiff CF1 1JW
Brazennose Street, Manchester M60 8AS
Southey House, Wine Street, Bristol BS1 2BQ
258 Broad Street, Birmingham B1 2HE
80 Chichester Street, Belfast BT1 4JY
Government Publications are also available through booksellers

C.P. No. 1331

ISBN 011 470941 6